

Detection of Landslide-Prone Areas in Garut Regency Using Composite Mapping Analysis and Geographic Information System

Ilham Badaruddin Mataburu^a, Lia Kusumawati^b and Ode Sofyan Hardi^c

Department of Geography, Universitas Negeri Jakarta, DKI Jakarta, Indonesia

Keywords: Landslide, CMA, GIS.

Abstract: Landslides represent one of the most frequent disasters in Garut Regency, resulting in various detrimental impacts, including property damage, infrastructure impairment, and even loss of life. Identifying areas susceptible to landslides can aid significantly in mitigation efforts. The objective of this study is to map these landslide-prone regions within Garut Regency. The research employs a Composite Mapping Analysis (CMA) model alongside Geographic Information System (GIS) technology, utilizing five parameters that influence landslide occurrences: land use, slope, geology, rainfall, and elevation, in addition to one parameter for comparing locations of previous landslides. The findings indicate that the CMA and GIS models, based on the five parameters utilized, effectively contribute to understanding landslide occurrences, as evidenced by the designated weight values of each parameter. Specifically, the geology, land use, and slope parameters exhibited high weight values of 30.29, 29.84, and 17.71, respectively, highlighting their significant role in landslide susceptibility in this region. The delineation of landslide-prone areas revealed that 9.99% of Garut Regency is classified as having very high vulnerability, while 16.18% falls into the high vulnerability category, predominantly located in the southern areas of the Cisompet, Pakenjeng, and Talegong sub-districts.

1 INTRODUCTION


Landslides are one of the most frequently occurring natural disasters in Indonesia, often resulting in significant loss of life and property. According to a report by BNPB (2020), there were 726 landslide incidents in 2019, leading to 114 fatalities and the evacuation of 12.193 people due to the destruction of homes. This marked an increase from the previous year, which recorded 642 landslide events that also resulted in casualties, injuries, and extensive damage to residential buildings and critical infrastructure.


Garut Regency is classified as a high-risk disaster area (BNPB, 2020), experiencing nine different types of disasters frequently. From 2015 to 2019, 41 landslides occurred in this region resulting in six fatalities and extensive damage to residential buildings, requiring the evacuation of 433 people. Landslides have also severely impacted critical infrastructure, including roads and bridges, as well as agricultural land. The high landslide risk in this


region is driven not only by geophysical factors but also by extensive land-use changes, as forest areas have been rapidly converted into agricultural land and residential areas over recent years.

Identifying landslide-prone areas is essential for effective disaster management. Efforts to reduce disaster impacts through prevention, mitigation, and adaptation strategies must begin with an understanding of landslide susceptibility based on the types of landslides across different landforms. Therefore, knowledge of landslide vulnerability is crucial (Mubekti & Fauziah, 2008; Susanti & Miardini, 2019).

The use of Geographic Information System (GIS) technology facilitates the identification of disaster-prone areas, and its application in mitigation efforts has been extensively studied. Developing GIS models integrated with statistical methods has proven highly accurate in detecting landslide susceptibility (Pasang & Kubicek, 2020). Integrating various landslide causative factors helps clarify the role of each

^a  <https://orcid.org/0009-0006-9338-1325>

^b  <https://orcid.org/0000-0001-8334-8229>

^c  <https://orcid.org/0009-0007-9691-5385>

indicator in influencing landslide potential (Mersha & Meten, 2020). This approach is crucial for decision-makers in formulating disaster-based spatial planning for prevention and mitigation purposes. Therefore, this study aims to map landslide-prone areas in Garut Regency using the Composite Mapping Analysis (CMA) model and GIS. This method is expected to assess the contribution of each landslide-driving factor both statistically and spatially

2 METHOD

2.1 Location

This research was conducted from May to September 2021 in Garut Regency, West Java Province. According to the administrative division, the Garut Regency consists of 42 subdistricts, 422 villages, and 21 urban villages.

2.2 Materials and Tools

The landslide-prone areas were analyzed using five parameters in the form of spatial data (maps), namely land use, slope, elevation, geology, and rainfall, as well as landslide location points as comparison parameters for determining weights and scores. The analysis of landslide-prone areas was conducted using Geographic Information System (GIS) software with overlay functions. The tools used in this study included GPS and ArcGIS 10.3 software.

2.3 Analysis Method

The landslide-prone areas were analyzed using the Geographic Information System (GIS) overlay method. The weighting and scoring for each parameter affecting landslide susceptibility were conducted using the Composite Mapping Analysis (CMA) model. The weights and scores for each parameter were determined by comparing the number of observed landslide events with the expected incidence of landslides in each region (Boonyanuphap et al., 2001; Haryani et al., 2012). The expected number of landslides represents the total number of landslides that should ideally occur within each area based on the area's total area. The CMA mathematical formula for mapping landslide-prone levels is as follows:

$$TRL = \sum_{i=1}^n (Wi \cdot Xi) \dots\dots\dots(1)$$

Where:

- TRL is the landslide susceptibility level,
- Wi is the weight of parameter i , and

- Xi is the score for parameter i .

The weight Wi is formulated as:

$$Wi = \frac{Mi}{\sum Mi} \dots\dots\dots(2)$$

Where:

- Mi is the average total observation for each landslide susceptibility factor, and
- Xi is the score for each factor within each parameter.

The score Xi is calculated as follow:

$$Xi = \left(\frac{Oi}{Ei} \right) \cdot \frac{100}{\sum (Oi/Ei)} \dots\dots\dots(3)$$

Where:

- Oi is the total observed landslide incidents, and
- Ei is the expected number of landslide incidents.

The weight and score results from the CMA model for each parameter were used as weights and scores in the GIS analysis. All weights and scores were then input as spatial data attributes for each parameter. The overlay method was used to combine all landslide-prone parameters, followed by determining the susceptibility levels for each landslide-prone area in the GIS environment. Landslide susceptibility levels were divided into five classes using the following equation:

$$I = \frac{c-b}{k} \dots\dots\dots(4)$$

Where:

- I is the class interval distance,
- c is the highest score total,
- b is the lowest score total, and
- k is the desired number of classes.

3 RESULT

The paper size must be set to A4 (210x297 mm). The document margins must be the following:

3.1 Score Values for Each Parameter

Each class within each parameter has a different influence on landslide occurrence. The influence value is measured through spatial comparison between the distribution of landslide points and the types and extents of each parameter, indicated by the score value.

3.1.1 Land Use

Based on Table 1, the highest number of landslide occurrences is found in dryland farming/garden land use types. These areas are typically cultivated by the

Table 1. Area and Score of Land Use Parameter (Source: Data processing, 2021).

| No. | Land use | Area (Ha) | Area (%) | Number landslide points | Score |
|-----|----------------------|------------|----------|-------------------------|-------|
| 1 | Settlement | 18.038,70 | 5.83 | 5 | 16.94 |
| 2 | Building | 1.09 | 0.00 | 0 | 0.00 |
| 3 | Forest | 63.714,43 | 20.58 | 1 | 1.12 |
| 4 | Mangrove forest | 32.09 | 0.01 | 0 | 0.00 |
| 5 | Fish pond | 17,31 | 0.01 | 0 | 0.00 |
| 6 | Grassland | 2.736,84 | 0.88 | 0 | 0.00 |
| 7 | Waterbody | 1.701,18 | 0.55 | 0 | 0.00 |
| 8 | Garden | 51.154,24 | 16.52 | 16 | 22.42 |
| 9 | Irrigated rice field | 7.285,86 | 5.58 | 3 | 12.44 |
| 10 | Rain-fed rice field | 40.353,45 | 13.03 | 10 | 17.76 |
| 11 | Shrubland | 56.312,02 | 18.19 | 12 | 15.27 |
| 12 | Dry field | 57.981,82 | 18.73 | 9 | 11.12 |
| 13 | Sand embankment | 270.40 | 0.09 | 0 | |
| | Total | 309.599,43 | 100.00 | 56 | 97.07 |

Table 2. Area and Score of Elevation Parameter (Source: Data processing, 2021)

| No. | Elevation | Area (Ha) | Area (%) | Number landslide points | Score |
|-----|-------------|-----------|----------|-------------------------|--------|
| 1 | <500 | 82665,08 | 26.70 | 19 | 34.06 |
| 2 | 500 - 1000 | 120470,95 | 38.91 | 20 | 24.60 |
| 3 | 1000 - 1500 | 79680,82 | 25.74 | 15 | 27.89 |
| 4 | 1500 - 2000 | 22037,01 | 7.12 | 2 | 13.45 |
| 5 | >2000 | 4745,57 | 1.53 | 0 | 0.00 |
| | Jumlah | 309599,43 | 100.00 | 56 | 100.00 |

community as horticultural gardens with seasonal crops. The root systems of these crops are not strong enough to bind the soil effectively. Similarly, rain-fed rice fields, which have shallow roots, also contribute to soil stability issues. These two types of land use have the highest scores in terms of their contribution to landslide occurrences in the Garut Regency. Other land use types with relatively high scores include shrubland and dry fields (see Table 1). The distribution of land use types and landslide points can be seen in Figure 2a.

3.1.2 Elevation

The highest number of landslide occurrences is found at elevations of 500–1000 meters above sea level (m asl) and below 500 m asl. Generally, landslides rarely occur at elevations above 1500 m asl. This is related to land interventions from human activities, which are typically conducted at elevations below 1500 m asl. Areas at elevations above 1500 m are seldom utilized. The highest scores based on spatial comparisons are found at elevations <500 m asl and at elevations of 1000–1500 m asl (see Table 2). These areas are

generally located in the southern part and represent the lowest areas within the study region. The spatial distribution of elevation classes and landslide points is presented in Figure 2b.

3.1.3 Rainfall

Rainfall plays an important role in landslide occurrences (Tajudin et al., 2018). The infiltration of water into the soil increases the soil mass and creates a friction plane on the bedrock, making it more slippery and causing the soil to become more prone to movement (Paimin et al., 2009). The rainfall data used in this study is the maximum daily rainfall, divided into two classes. Based on the spatial comparison calculations, both rainfall classes show close score values (see Table 3). The higher score is found in the rainfall class of 13.6–20.7 mm, with a score of 50.25. This value does not differ significantly from the score in the 20.7–27.7 mm class, which is 49.75. The distribution of rainfall classes and landslide points is presented in Figure 2c.

Table 3. Area and Score of Rainfall Parameter (Source: Data processing, 2021)

| No. | Rainfall (mm/hr) | Area (Ha) | Area (%) | Number landslide points | Score |
|-------|------------------|------------|----------|-------------------------|--------|
| 1 | 13.6 – 20.7 | 192.768,91 | 62.26 | 35 | 50.25 |
| 2 | 20.7 – 27.7 | 116.830,52 | 37.74 | 21 | 49.75 |
| Total | | 309.599,43 | 100.00 | 56 | 100.00 |

Table 4. Area and Score of Slope Parameter (Source: Data processing, 2021)

| No. | Slope | Area (Ha) | Area (%) | Number landslide points | Score |
|-----|-----------|------------|----------|-------------------------|--------|
| 1 | 0 - 8 % | 50.209,94 | 16.2 | 1 | 2.41 |
| 2 | 8 - 15 % | 51.824,67 | 16.74 | 3 | 6.99 |
| 3 | 15 - 25 % | 70.362,27 | 22.73 | 15 | 25.75 |
| 4 | 25 - 40 % | 73.192,59 | 23.64 | 21 | 34.66 |
| 5 | >40% | 64.009,96 | 20.68 | 16 | 30.19 |
| | Total | 309.599,43 | 100.00 | 56 | 100.00 |

3.1.4 Slope

Based on the slope, the study area is mostly mountainous, with slopes greater than 15%. The central to northern areas, as well as the southern coastal area, are narrow plains with slopes of less than 15%. Landslide occurrences are found on slopes greater than 15%, with the highest number of occurrences in the 25–40% slope class. Based on spatial comparison, the highest scores are in the 25–40% and >40% slope classes. Score comparisons show that the highest scores are in areas with slope classes of 25–40% and >40%, with 21 and 16 landslide points, respectively. Subsequently, the score decreases with decreasing slope class. The score values and slope class distribution are presented in Table 4 and Figure 2d.

3.1.5 Geology

Geology is related to soil stability in terms of landslide potential; geological formations that are less compact are more likely to detach and experience soil movement, while more compact rocks tend to be more resistant to soil movement which can lead to landslides. Generally, the potential for soil movement is associated with the properties of rocks in responding to water or vibrations as landslide triggers (Paimin et al., 2009). Geologically, the study area is divided into 30 types of geological formations, most of which are volcanic in origin, consisting of volcanic rocks. The study area is dominated by tuff and breccia rocks, pyroclastic deposits, and young volcanic rocks, which are primarily found in the central to southern

parts of the study area (see Figure 2e). The score values from the CMA analysis through spatial comparisons between landslide points and geological types indicate that out of 30 geological types in the study area, only 7 contain landslide points with varying numbers. The highest scores are found in reef limestone and tuff and breccia members, with values of 25.46 and 21.14, respectively. Other geological types with relatively high scores include young volcanic rocks, old volcanic breccia, and pyroclastic deposits (see Table 5).

3.2 Weight of Each Parameter

Calculations using the CMA and SIG models, according to Equation 2, yield the weight values for each parameter in relation to its correlation with the distribution of landslide occurrences. The weight of each parameter correlates with the contribution of each parameter to landslide occurrences, and the results indicate that geology, land use, and slope gradient parameters exhibit the highest weight values.

3.2.1 Delineation of Landslide Hazard Areas

Landslide hazard levels were calculated using GIS by applying Equation 1 across all parameters, including land use, slope, rainfall, elevation, and geology. The analysis was conducted through overlay processes and mathematical operations on the weight and score values according to the equation below:

$$\text{TRL} = 29.84 \text{ SPL} + 17.71 \text{ SLE} + 7.73 \text{ SCH} + 30.29 \text{ SGE} + 14.43 \text{ SEle}$$

Where:

Table 5. Area and Score of Geology Parameter (Source: Data processing, 2021)

| No. | Geology type | Area (Ha) | Area (%) | Number of landslide points | Score |
|-------|---|------------|----------|----------------------------|--------|
| 1 | Breccia from old volcanic rocks | 23.377,73 | 7.55 | 5 | 15.10 |
| 2 | Lava from old volcanic rocks | 588,56 | 0.19 | 0 | 0.00 |
| 3 | Breccia from old volcanic products | 1.175,29 | 0.38 | 0 | 0.00 |
| 4 | Unaltered old volcanic products | 16.10 | 0.01 | 0 | 0.00 |
| 5 | Mandalawangi-Mandalagi volcanic formation | 1.693,12 | 0.55 | 0 | 0.00 |
| 6 | Pumice tuff and breccie | 2.228,47 | 0.72 | 0 | 0.00 |
| 7 | Sangianganjung volcanic rocks | 156,11 | 0.05 | 0 | 0.00 |
| 8 | Guntur-Pangkalan volcanic rocks | 12.648,52 | 4.09 | 1 | 5.58 |
| 9 | Young volcanic rocks | 61.388,69 | 19.83 | 15 | 17.25 |
| 10 | Loose recent sediments | 16.918,58 | 5.46 | 0 | 0.00 |
| 11 | Lava guntur | 3.578,22 | 1.16 | 0 | 0.00 |
| 12 | Kolovial | 102,83 | 0.03 | 0 | 0.00 |
| 13 | Olf volcanic efflata deposits | 2.019,79 | 0.65 | 0 | 0.00 |
| 14 | Alluvial | 8.311,41 | 2.68 | 0 | 0.00 |
| 15 | Old volcanic products | 7.239,49 | 2.34 | 0 | 0.00 |
| 16 | Papandayan volcanic efflata | 3.821,86 | 1.23 | 0 | 0.00 |
| 17 | Waringin-Bedil Andesite | 6.064,75 | 1.96 | 0 | 0.00 |
| 18 | Intrusive rocks | 3.461,63 | 1.12 | 0 | 0.00 |
| 19 | Koleberes formation | 1.881,78 | 0.61 | 0 | 0.00 |
| 20 | Pyroxene andesite | 88,67 | 0.03 | 0 | 0.00 |
| 21 | Pyroclastic deposits | 45.556,77 | 14.71 | 7 | 10.85 |
| 22 | Tuff and breccia members | 86.839,23 | 28.05 | 26 | 21.14 |
| 23 | Benteng formation | 15.308,18 | 4.94 | 1 | 4.61 |
| 24 | Lower benteng formation | 61,21 | 0.02 | 0 | 0.00 |
| 25 | Quartz diorite | 116,87 | 0.04 | 0 | 0.00 |
| 26 | Jampang formation | 1.788,07 | 0.58 | 0 | 0.00 |
| 27 | Alluvial dan coastal deposits | 149.04 | 0.05 | 0 | 0.00 |
| 28 | Andesite | 197.62 | 0.06 | 0 | 0.00 |
| 29 | Andesite hornblende | 47.68 | 0.02 | 0 | 0.00 |
| 30 | Coral reef limestone | 2.773,14 | 0.90 | 1 | 25.46 |
| Total | | 309.599,43 | 100.00 | 56 | 100.00 |

- TRL represents the landslide hazard level,
- SPL is the score for the land use parameter,
- SLE is the score for the slope parameter,
- SCH is the score for the rainfall parameter,
- SGE is the score for the geology parameter,
- and

- SEle is the score for the elevation parameter.
- The calculation results showed a minimum value of 431,11 and a maximum value of 2.844, 91. Subsequently, the landslide hazard levels are divided into 5 classes following Equation 5 as follows:

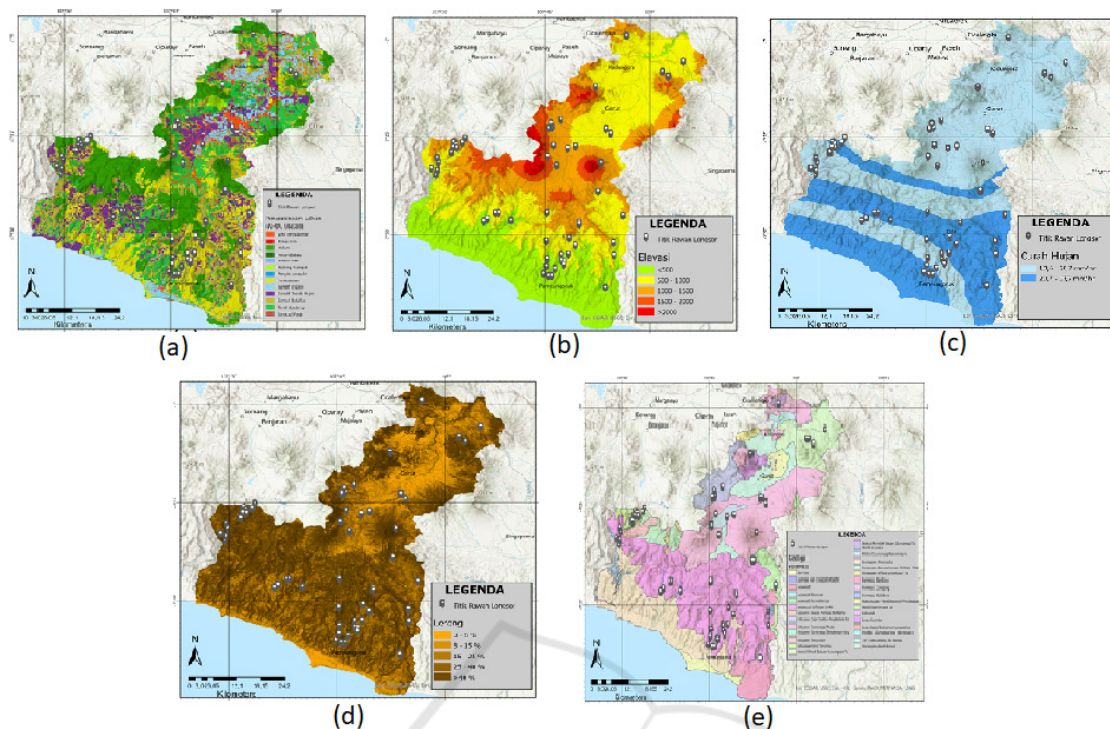


Figure 2: Map of (a) Land use; (b) Elevation; (c) Rainfall; (d) Slope; (e) Geology.

Table 6. Weight of Landslide Parameter

| No | Parameter | Weight |
|-------|-----------|--------|
| 1 | Land use | 29.84 |
| 2 | Slope | 17.71 |
| 3 | Rainfall | 7.73 |
| 4 | Geology | 30.29 |
| 5 | Elevation | 14.43 |
| Total | | 100.00 |

Source: Data processing, 2021

Table 7. Landslide Hazard Class (Source: Data analysis, 2021)

| Landslide Hazard Class | TRL Value |
|------------------------|-------------------|
| Very low | < 913.87 |
| Low | 913.87 - 1396,63 |
| Moderate | 1396,63 - 1879,39 |
| High | 1879,39 - 2362,15 |
| Very high | > 2362,15 |

According to Table 7, areas with a very low landslide hazard level constitute the largest area in the Garut Regency, while areas with a very high hazard level represent the smallest area (9.99%). These high-hazard areas are generally distributed from the southern to central parts and on the left side near the

border between Garut and Tasikmalaya Regencies. This region consists of southern limestone hills and areas surrounding the central and eastern volcanic mountains in Garut Regency. It typically features steep slopes and high rainfall, especially in mountainous areas approaching borders with neighboring regencies (see Figure 3).

The largest extent of very high hazard areas is primarily found in Cisompet District, with significant areas also in Cikelet District, Pakenjeng District, and partially in Bungbulang and Banjarwangi Districts. Similarly, high-hazard areas are concentrated in Cisompet and Pakenjeng, which have the largest land area in this category.

3.3 Discussion

The use of CMA and GIS models in landslide hazard mapping, employing five determining parameters and comparing them with landslide occurrence data, effectively identifies areas with similar characteristics across the five parameters and assesses their hazard levels both statistically and spatially. The application of GIS and the CMA model indicates that landslide occurrences in Garut Regency are influenced by specific factors: geological types of tuff and breccia, land use for plantations, slopes between 5–40% and greater than 40%, elevations of 500–1000

Table 8. Landslide Hazard Area in Garut Regency (Source: Data analysis, 2021)

| No | Landslide Hazard Level | Area (ha) | Area (%) |
|-------|------------------------|------------|----------|
| 1 | Not hazardous | 130.145,85 | 42.04 |
| 2 | Slightly hazardous | 52.132,34 | 16.84 |
| 3 | Moderately hazardous | 46.295,13 | 14.95 |
| 4 | Hazardous | 50.094,38 | 16.18 |
| 5 | Very hazardous | 30.931,73 | 9.99 |
| Total | | 309.599,43 | 100.00 |

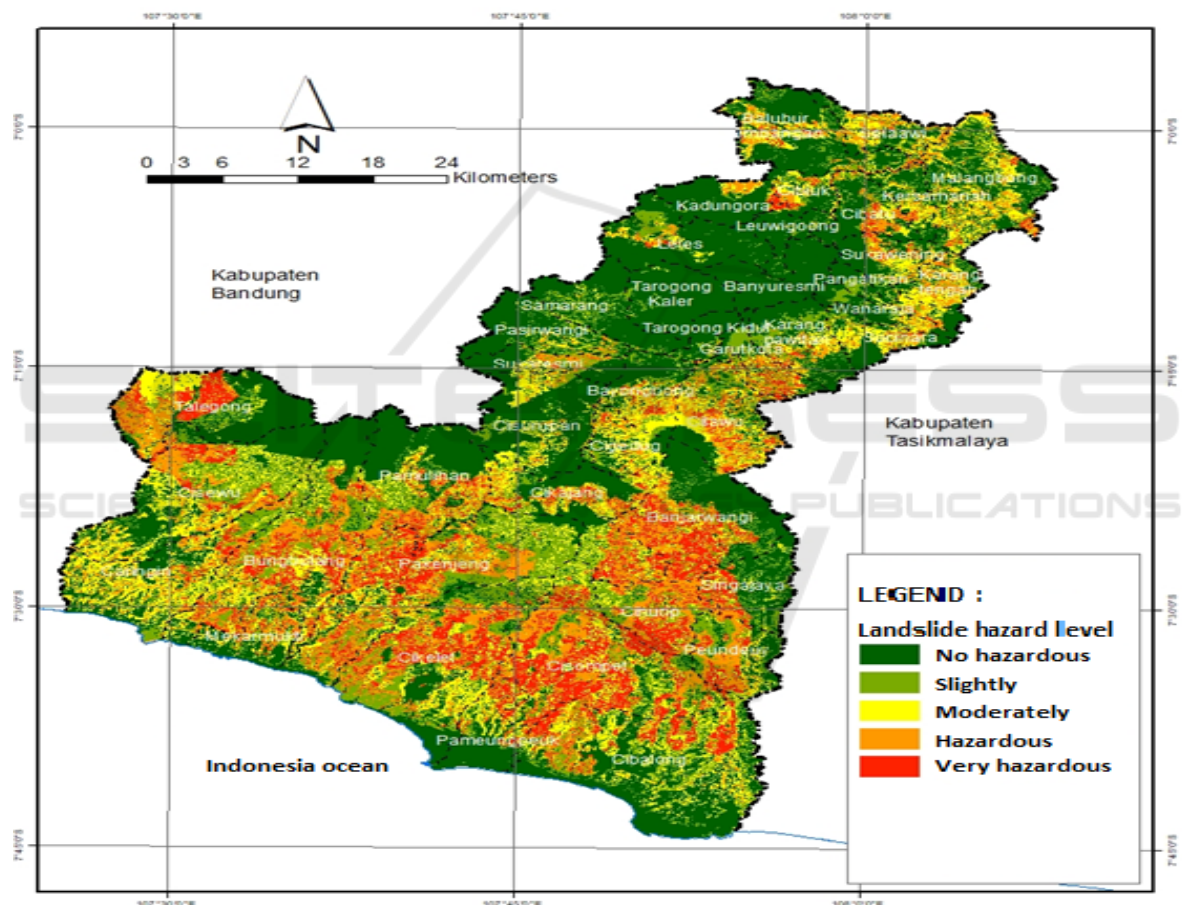


Figure 3: Map of Landslide Hazardous in Garut Regency.

meters, and a generally even distribution concerning rainfall.

Geology and land use are parameters closely associated with landslide occurrences (Faizana et al., 2015; Pasang & Kubicek, 2020). Research findings indicate that these two parameters have the highest weights based on landslide distribution in Garut Regency. Landslide distribution is concentrated in

areas with geological types such as tuff and breccia and young volcanic rocks, both of which formed from past volcanic activity, particularly in the central to northern regions (Sulaksana et al., 2014). The southern part consists of karst hills, featuring varied topography with steep to very steep slopes. Rock layers that allow water to seep until reaching

impermeable layers can trigger slippage, leading to landslides (Paimin et al., 2009).

Another determining factor for landslide occurrences in the study area is land use, which relates to the land's ability to respond to water. Landslides commonly occur on agricultural lands, such as fields and dryland farms. The incidence of landslides increases with the rapid change in land use in this region, as Garut Regency is among the areas with a high rate of land-use change, especially around slopes and the foothills of volcanic mountains, which are fertile for horticulture or seasonal crops like corn, cabbage, scallions, and other vegetables (Muldiana et al., 2016). Intensive land-use changes, driven by infrastructure development or agricultural expansion, can increase landslide potential (Moresi et al., 2020; Pasang & Kubicek, 2020). Agricultural activities in Garut Regency occur on various topographies, with dryland farming spread across hills and the foothills to the slopes of mountains, including areas with slopes > 25%. This situation disrupts soil stability and potentially increases landslide occurrences (Anbalagan et al., 2015). The type of land use affects slope stability, as seasonal agricultural lands with shallow-rooted crops decrease slope stability, increasing the risk of landslides (Susanti & Miardini, 2019). Landslide events in Garut Regency primarily occur on slopes > 25%, with land uses such as plantations, fields, and shrublands.

4 CONCLUSIONS

The study produced several conclusions:

1. The use of GIS and the CMA model effectively maps landslide hazard areas by comparing five determining parameters with the landslide occurrence parameter through weighting and scoring of each parameter.
2. Geological factors, land use, and slope are the parameters with the highest contribution to landslide occurrences in Garut Regency.
3. The distribution of high and very high landslide hazard areas is generally located in the southern to central parts of Garut Regency, which consist of a series of hills and mountains, primarily in Cisompet and Pakenjen Districts. Areas classified as relatively non-hazardous to slightly hazardous are typically found in the central to northern and western regions, which have gentler slopes, including Garut Kota, Tarogong Kidul, Tarogong Kaler, and Banyuresmi Districts.

RECOMMENDATIONS

The resulting landslide hazard map can serve as a consideration in spatial planning as an initial step to determine the type and location of land use allocation as part of landslide disaster mitigation efforts in the Garut Regency. For future research, the use of the CMA model and GIS relies heavily on the number and types of parameters applied. Additional parameters should be included to obtain improved results.

REFERENCES

- Anbalagan, R., Kumar, R., Lakshmanan, K., Parida, S., & Neethu, S. (2015). Landslide hazard zonation mapping using frequency ratio and fuzzy logic approach, a case study of Lachung Valley, Sikkim. *Geoenvironmental Disasters*, 2(6), 1–17. <https://doi.org/10.1186/s40677-014-0009-y>
- Boonyanuphap, J., Suratmo, F. G., & Jaya, I. N. S. (2001). Gis-based method in developing wildfire risk model (Case study in Sasamba, East Kalimantan, Indonesia). *Jurnal Manajemen Hutan Tropika*, 7(2), 33–45. <https://doi.org/10.7226/jmht.7.2>
- Faizana, F., Nugraha, A. L., & Yuwono, B. D. (2015). Pemetaan risiko bencana tanah longsor Kota Semarang. *Jurnal Geodesi Undip*, 4(1), 223–234.
- Haryani, N. S., Zubaidah, A., Dirgahayu, D., Hidayat, F. Y., & Junita, P. (2012). Model bahaya banjir menggunakan data penginderaan jauh di Kabupaten Sampang. *Jurnal Penginderaan Jauh*, 9(1), 52–66.
- Mersha, T., & Meten, M. (2020). *GIS-based landslide susceptibility mapping and assessment using bivariate statistical methods in Simada area, northwestern*.
- Moresi, F. V., Maesano, M., Collalti, A., Sidle, R. C., Matteucci, G., & Mugnozza, G. S. (2020). Mapping Landslide Prediction through a GIS-Based Model: A Case Study in a Catchment in Southern Italy. *Geosciences*, 10(309), 1–22. <https://doi.org/doi:10.3390/geosciences10080309>
- Mubekti, M., & Fauziah, A. (2008). Mitigasi Daerah Rawan Tanah Longsor Menggunakan Teknik Pemodelan Sistem Informasi Geografis; Studi Kasus: Kecamatan Sumedang Utara dan Sumedang Selatan. *Jurnal Teknik Lingkungan*, 9(2), 121–129.
- Muldiana, A., Sugandi, D., & Somantri, L. (2016). Pemanfaatan citra landsat 8 untuk analisis penggunaan lahan di Kabupaten Garut. *Antologi Pendidikan Geografi*, 4(2), 73–80. <http://journal.ikipgriptk.ac.id/index.php/edukasi/articledownload/17/16>
- Paimin, Sukresno, & Pramono, I. B. (2009). *Teknik Mitigasi Banjir dan Tanah longsor* (A. N. Ginting (ed.)). Tropenbos International Indonesia Programme.
- Pasang, S., & Kubicek, P. (2020). Landslide Susceptibility Mapping Using Statistical Methods along the Asian

- Highway, Bhutan. *Geosciences*, 10(430), 1–26.
<https://doi.org/10.3390/geosciences10110430>
- Pellicani, R., Argentiero, I., Spilotro, G., Argentiero, I., & Spilotro, G. (2017). GIS-based predictive models for regional-scale landslide susceptibility assessment and risk mapping along road corridors susceptibility assessment and risk mapping along road corridors. *Geomatics, Natural Hazards and Risk*, 5705. <https://doi.org/10.1080/19475705.2017.1292411>
- Sulaksana, N., Sukiyah, E., Sjafrudin, A., & Haryanto, E. T. (2014). Karakteristik geomorfologi DAS Cimanuk bagian hulu dan implikasinya terhadap intensitas erosi serta pendangkalan Waduk Jatigede. *Bionatura-Jurnal Ilmu-Ilmu Hayati Dan Fisik*, 16(2), 95–102.
- Susanti, P. D., & Miardini, A. (2019). *Identifikasi Karakteristik dan Faktor Pengaruh pada Berbagai Tipe Longsor*. 39(2), 97–107.
- Tajudin, N., Ya'acob, N., Ali, D. M., Adnan, N., & Naim, N. F. (2018). Rainfall – landslide potential mapping using remote sensing and GIS at Ulu Kelang , Selangor , Malaysia. *IOP Conference Series: Earth and Environmental Science*, 012080, 1–8. <https://doi.org/doi:10.1088/1755-1315/169/1/012080>

